Ecography

ECOG-04403
Vidal, M. M., Banks-Leite, C., Tambosi, L. R., Hasui, È., Develey, P. F., Silva, W. R., Guimarães Jr, P. R. and Metzger, J. P. 2019. Predicting the non-linear collapse of plant-frugivore networks due to habitat. – Ecography
doi: 10.1111/ecog.04403

Supplementary material

APPENDIX A. Relationship between minimum percentage of habitat cover and independent assessments of bird extinction proneness

Here we detailed the methods used to evaluate the relationship between the minimum percentages of habitat cover where each bird species was recorded and (i) its sensitivity to human disturbances (Stotz et al. 1996); and (ii) its level of habitat specialization (De Coster et al. 2015), variables that may be indicative of extinction proneness.

Stotz et al. (1996) assigned each Neotropical bird species a qualitative assessment of sensitivity to human disturbances (high, medium or low). We tested the relationship between bird sensitivity to human disturbances and minimum percentage of habitat cover by performing two-sample randomization tests (Manly 1997), comparing the three categories of bird sensitivity (high x medium; high x low; and medium x low). For each comparison, we randomized the minimum percentages of habitat cover among the levels of sensitivity to human disturbances (1000 replicates). We found significant differences between categories of sensitivity to human disturbances with respect to their minimum percentages of habitat cover: high sensitivity x low sensitivity: $P < 0.001$; high sensitivity x medium sensitivity: $P = 0.029$; medium sensitivity x low sensitivity: $P < 0.001$ (Fig. A1).

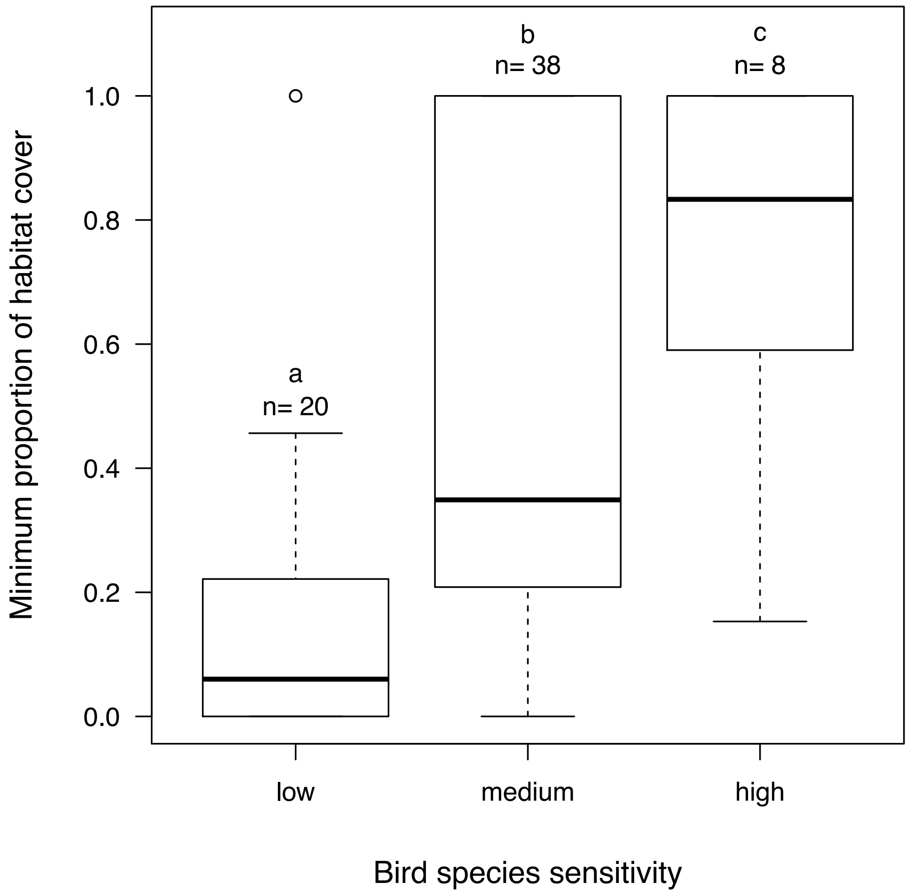

Figure A1. Relationship between minimum proportion of forest cover around sample points where each bird species was recorded (our proxy for species proneness to extinction due to habitat loss) with bird species levels of sensitivity to human disturbances. Different upper letters show significant differences between sensitivity categories.

We used a second validation of our hypothesis that birds restricted to larger amounts of habitat would be extinct first. We explored the relationship between the minimum percentage of habitat cover where each species was recorded and level of habitat specialization. Habitat specialists tend to be more vulnerable to habitat loss than habitat generalist species (Owens and Bennett 2000, Fischer and Lindenmayer 2007). So, we classified all the bird species from our networks with respect to their degree of habitat specialization. We used information on the types of habitats in which each bird species lives (Stotz et al. 1996) to derive an index of habitat specialization (*HS*), following De Coster et al. (2015):

$$HS = 1 - \frac{x + y - 1}{\max(x + y - 1)},$$

where x is the total number of habitats, and y equals 1 if the bird species occurs in forest and non-forest habitats (0 if the bird species occurs only in forest habitats). Thus, the parameter y reduces *HS* values for species that occur in both forest and non-forest habitats, whereas it increases *HS* values for species restricted to forested physiognomies. Habitat specialization values range between 0–1, with specialists having higher values than generalists. We tested for the association between minimum proportions of habitat cover where each bird species was recorded and their degree of habitat specialization by performing linear regression analysis. We found a positive relationship between habitat specialization and minimum proportion of habitat cover (R-squared = 0.21, $P < 0.001$; Fig. A2).

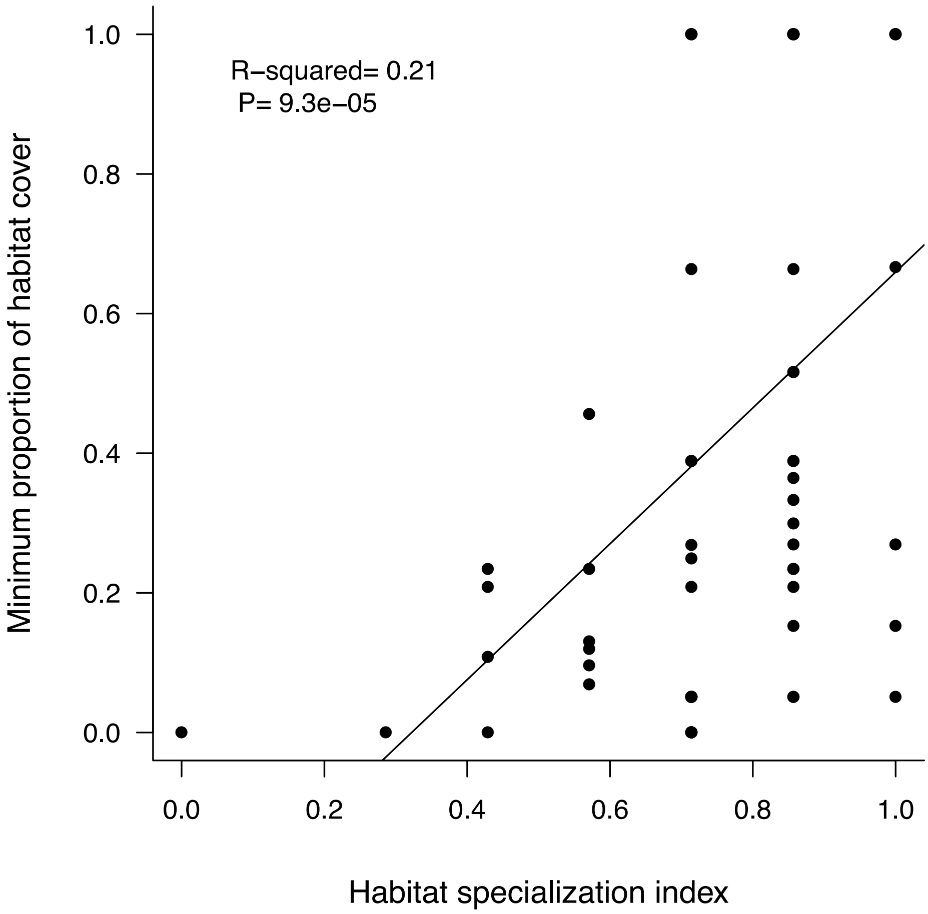

Figure A2. Relationship between minimum proportion of forest cover around sample points where each bird species was recorded (our proxy for species proneness to extinction due to habitat loss) with bird species specialization in habitat use.

References

De Coster, G. et al. 2015. Atlantic forest bird communities provide different but not fewer functions after habitat loss. – Proc. R. Soc. B. 282: 20142844.

Fischer, J. and Lindenmayer, D. B. 2007. Landscape modification and habitat fragmentation: a synthesis. – Glob. Ecol. Biogeogr. 16: 265–280.

Manly, B. F. J. 1997. Randomization, Bootstrap and Monte Carlo Methods in Biology. 2nd edition. – Chapman & Hall/CRC.

Owens, I. P. F. and Bennett, P. M. 2000. Ecological basis of extinction risk in birds: habitat loss versus human persecution and introduced predators. – Proc. Natl. Acad. Sci. U. S. A. 97: 12144.

Stotz, D. F. et al. 1996. Neotropical birds: ecology and conservation. – University of Chicago Press, Chicago.

APPENDIX B. Species's contribution to network structure, modularity analysis and sampling completeness

Here we detailed methods on how we computed each species' contribution to network structure, network modularity and sampling completeness.

We computed the contribution of each bird species to the structure of the three studied networks, as well as for the network that combines data from the three sites (combined network), by combining several descriptors of their structural role: their number of interactions (k_i), standardized within-module degree (z_i), among-module connectivity (c_i) and contribution to nestedness (n_i) (Vidal et al. 2014). The metrics z_i and c_i are two topological properties associated to modularity of the network. Modularity is a pattern of interaction describing the organization of species in interconnected groups (modules), in which they interact more among themselves than with species from other groups (Olesen et al. 2007). Standardized within-module degree (z_i) is a standardized measure of the extent to which each species is connected to the others in its own module. Among-module connectivity (c_i) describes how well each species is connected to species in other modules. Contribution of each species to nestedness (n_i) is based on the metric NODF (Almeida-Neto et al. 2008) and it describes how each species share partners with more generalized species. Details on computing z_i, c_i and n_i are available elsewhere (Olesen et al. 2007, Vidal et al. 2014). For all bird species comprised in each network, we performed a Principal Component Analysis (PCA) on the correlation matrix among k_i, n_i, z_i and c_i normalized values. We used the first principal component to synthesize the species contributions to connectivity, nestedness, and modularity in one descriptor of its structural role, which we refer to as the contribution of each bird species to network structure (Vidal et al. 2014). We performed PCA using R software (R Core Team

2017). We then investigated how the contribution to network structure was distributed among classes of minimum percentages of habitat cover where each bird species was recorded: species recorded in areas with at least 40% of forest cover, species in areas between 30% and 40% of forest cover, and species in areas with less than 30% of forest cover. Such categorization allowed pooling species with similar

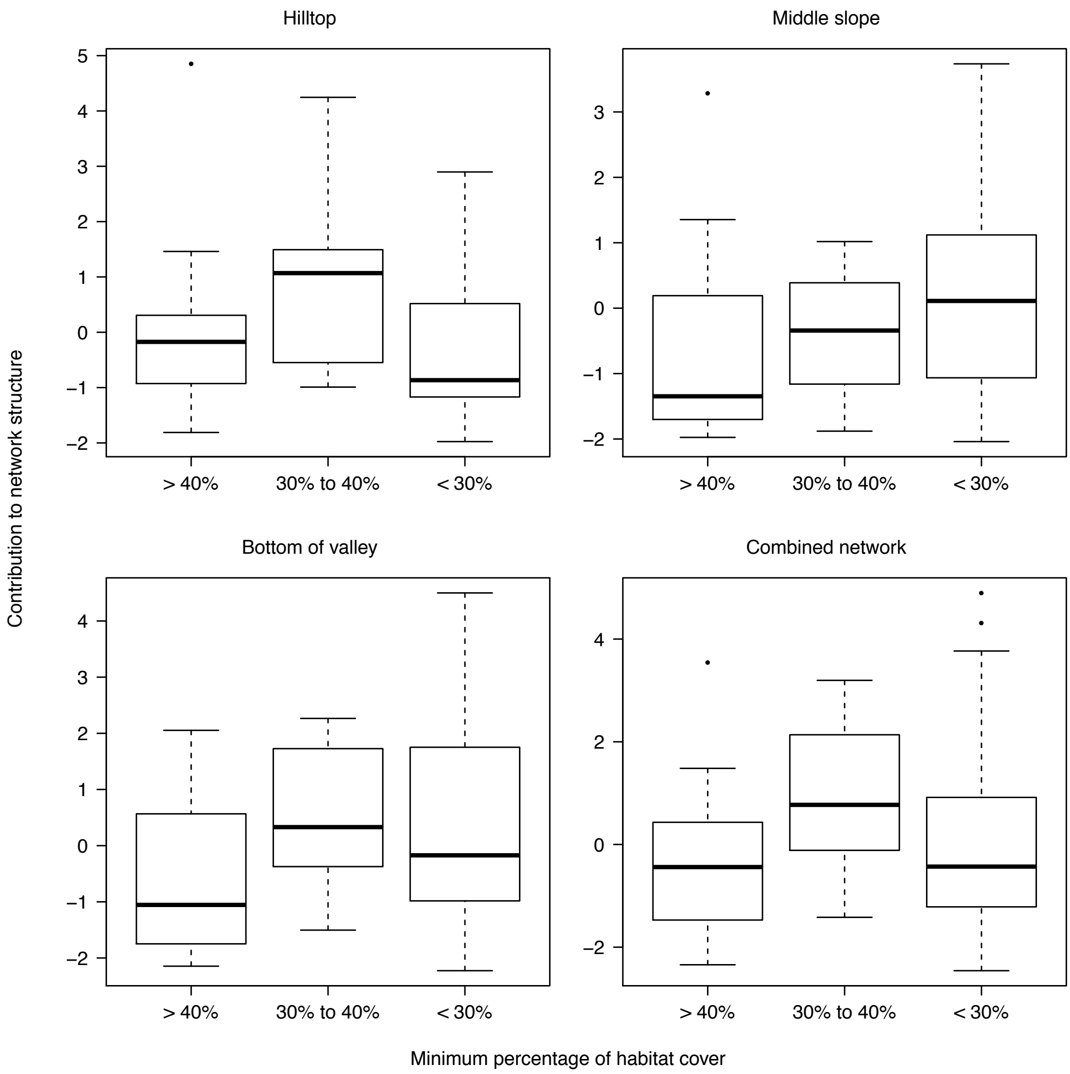

area requirements, generating some variation inside each percentage category.

Figure B1. Variation in bird species contribution to network structure (hilltop, middle slope, bottom of valley and combined network) within each category of minimum percentage of habitat cover.

For each studied network, we assessed network modularity by computing the metric *Q* (Newman and Girvan 2004), using simulated annealing as the optimization algorithm to search for the partition of the network into modules that maximizes the modularity index. To evaluate if heterogeneity in number of interactions would suffice to reproduce the observed modularity in our networks, we compared the observed modularity with the modularity values of 100 replicates generated by a null model that keeps the original distribution of links per node (null model 2 in Bascompte et al. 2003). For all modularity analyses we used the software MODULAR (Marquitti et al. 2014).

We calculated sampling completeness following Ramírez-Burbano et al. (2017). In this approach, each plant-frugivore combination is considered as a species and the frequency of each pairwise interaction is seen as their abundances. With these data, we computed the Chao 1 estimator of species richness to estimate the total number of interactions in the community. We opted for Chao 1 estimator, an estimator of species richness for abundance data, because we had data on the frequency of interactions, not only incidence data. We used the iNEXT package (Hsieh et al. 2019) in R (R Core Team 2017) to compute Chao 1 estimator. Then, we calculated sampling completeness by dividing the observed number of interactions by the estimated number of interactions given by Chao 1 (Chacoff et al. 2012).

References

Almeida-Neto, M. et al. 2008. A consistent metric for nestedness analysis in ecological systems: reconciling concept and measurement. - Oikos 117: 1227–1239.

Bascompte, J. et al. 2003. The nested assembly of plant–animal mutualistic networks. - Proc. Natl. Acad. Sci. U. S. A. 100: 9383–9387.

Chacoff, N. P. et al. 2012. Evaluating sampling completeness in a desert plant–pollinator network. - J. Anim. Ecol. 81: 190–200.

Hsieh, T. C. et al. 2019 iNEXT: iNterpolation and EXTrapolation for species diversity. R package version 2.0.19 URL: http://chao.stat.nthu.edu.tw/blog/software-download/.

Marquitti, F. M. D. et al. 2014. MODULAR: software for the autonomous computation of modularity in large network sets. - Ecography 37: 221–224.

Newman, M. E. J. and Girvan, M. 2004. Finding and evaluating community structure in networks. - Phys. Rev. E 69: 026113.

Olesen, J. M. et al. 2007. The modularity of pollination networks. - Proc. Natl. Acad. Sci. U. S. A. 104: 19891–19896.

R Core Team. 2017. R: A language and environment for statistical computing. R Foundation for Statistical Computing, Vienna, Austria. Available at: www.R-project.org.

Ramírez‐Burbano, M. B. et al. 2017. The role of the endemic and critically endangered Colorful Puffleg *Eriocnemis mirabilis* in plant-hummingbird networks of the Colombian Andes. - Biotropica 49: 555–564.

Vidal, M. M. et al. 2014. Frugivores at higher risk of extinction are the key elements of a mutualistic network. - Ecology 95: 3440–3447.

APPENDIX C. Predicted frugivory network parameters for the Serra do Mar bioregion: current status of the best-preserved Atlantic Forest area

Estimating current forest cover

To estimate the current forest cover in the Atlantic Forest biome we used the 2016 land cover data from MapBiomas v. 2.3 (Project MapBiomas 2018) available in a 30 m spatial resolution. First we reclassified the land cover classes into forest (native forest cover classes) and non-forest (all other land cover classes) and then we calculated the percentage of forest cover in 800 m radius using a moving window approach. Then, we resampled the percentage of forest cover raster to a 1600 m spatial resolution to avoid computational problems when extrapolating the piecewise regression models.

Extrapolating frugivory network metrics to Serra do Mar bioregion

From our linear piecewise regression model designed for the combined network, we predicted values of network metrics that would be expected for the current percentages of forest cover found in the Serra do Mar bioregion. Then, we calculated the cumulative percentage of the bioregion bellow the forest cover thresholds identified for each network structure metric. We extrapolated the network structure metrics only to the Serra do Mar bioregion because all of our studied sites are in this bioregion and it is climatic and biologically different from other Atlantic Forest bioregions (Silva and Casteleti 2003, Ribeiro et al. 2011).

Here we present the predicted values of number of species (Fig. C1), number of interactions (Fig. C2), connectance (Fig. C3) and nestedness (Fig. C4). For each network metric, we highlight the predicted value when forest cover equals the estimated breakpoint, and the corresponding proportion of the bioregion that is below such breakpoint.

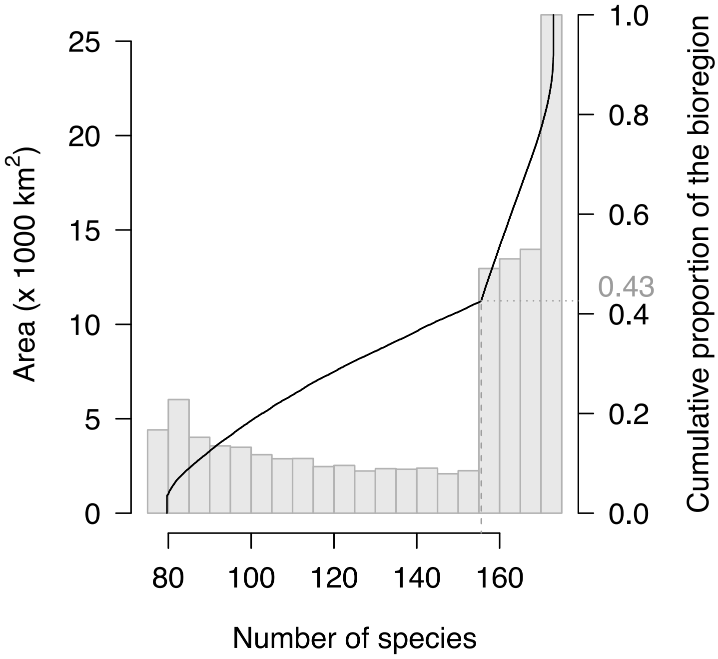

Figure C1. Histogram of the area (bars) and cumulative proportion of the Serra do Mar bioregion (solid line) within classes of number of species predicted for frugivory networks, according to forest cover. We highlight the number of species (155.57) predicted for 39% of forest cover (the estimated breakpoint), and corresponding proportion of the Serra do Mar bioregion (0.43) that shows lower values of number of species.

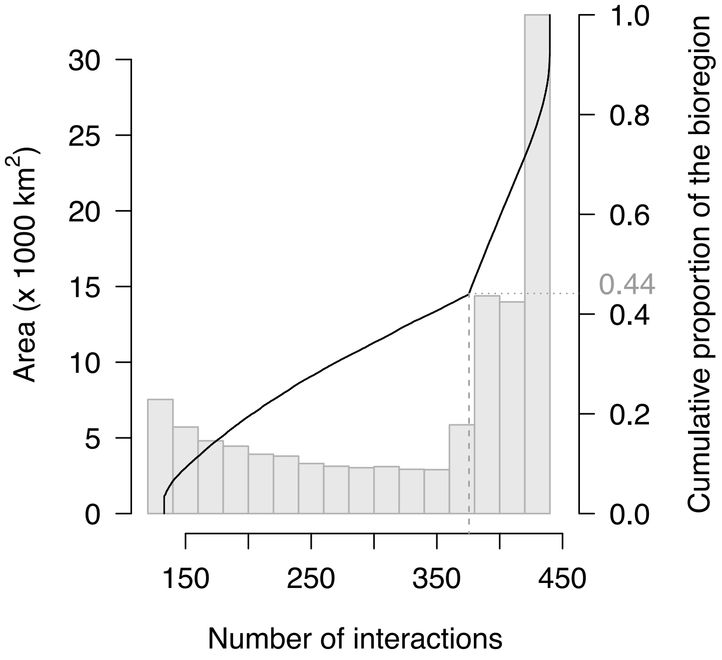

Figure C2. Histogram of the area (bars) and cumulative proportion of the Serra do Mar bioregion (solid line) within classes of number of interactions predicted for frugivory networks, according to forest cover. We highlight the number of interactions (375.59) predicted for 41% of forest cover (the estimated breakpoint), and corresponding proportion of the Serra do Mar bioregion (0.44) that shows lower values of number of interactions.

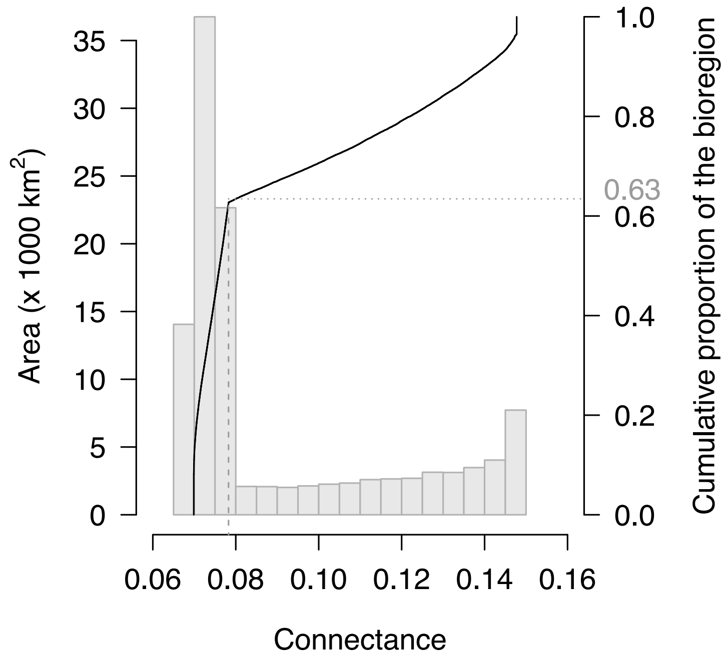

Figure C3. Histogram of the area (bars) and cumulative proportion of the Serra do Mar bioregion (solid line) within classes of connectance values predicted for frugivory networks, according to forest cover. We highlight the connectance (0.078) predicted for 32% of forest cover (the estimated breakpoint), and corresponding proportion of the Serra do Mar bioregion (0.63) that shows lower values of connectance. In other words, 37% of the bioregion shows greater values of connectance, as the trend is connectance to increase after forest cover reaches the threshold (see main text).

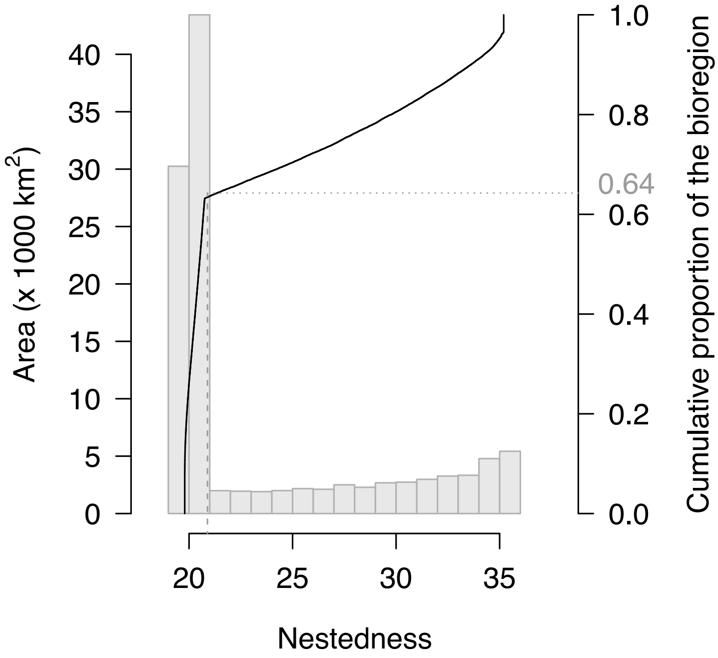

Figure C4. Histogram of the area (bars) and cumulative proportion of the Serra do Mar bioregion (solid line) within classes of nestedness values predicted for frugivory networks, according to forest cover. We highlight the nestedness (20.89) predicted for 31% of forest cover (the estimated breakpoint), and corresponding proportion of the Serra do Mar bioregion (0.64) that shows lower values of nestedness. In other words, 36% of the bioregion shows greater values of nestedness, as the trend is nestedness to increase after forest cover reaches the threshold (see main text).

References

Ribeiro, M. C. et al. 2011. The Brazilian Atlantic Forest: A Shrinking Biodiversity Hotspot. –In: Zachos, F. E. and Habel, J. C. (eds). Biodiversity Hotspots:

distribution and protection of conservation priority areas. Springer-Verlag Berlin Heidelberg.

Silva, J. M. C. and Casteleti, C. H. M. 2003. Status of the biodiversity of the Atlantic Forest of Brazil. –In: Galindo-Leal, C. and Câmara, I. G. (eds). The Atlantic Forest of South America: biodiversity status, threats, and outlook. CABS and Island Press, Washington, D.C., USA, pp. 43–59.

APPENDIX D. **Tables containing network structure descriptors (Table D1), list of bird species and respective minimum percentages of forest cover in the sites where they were recorded (Table D2) and threshold estimates in the response of network structure to habitat loss (Table D3)**

Table D1. Descriptors of the three plant-frugivore interaction networks (hilltop, middle slope, and bottom of valley) from a well-preserved Atlantic Forest remnant in southeastern Brazil and the network that combines data from the three sites.

Descriptor	**Hilltop**	**Middle slope**	**Bottom of valley**	**Combined network**
Species richness				
Birds	43	37	47	67
Plants	54	55	71	127
Mean number of interactions				
Birds	3.70	4.05	5.13	7.90
Plants	2.94	2.73	3.39	4.17
Connectance	0.07	0.07	0.07	0.06
Nestedness (NODF)	16.31	18.27	18.58	17.93
Modularity (Q)	0.54	0.52	0.45	0.39

Table D2. Bird species comprised in the network that combines data from three sites inside Parque Estadual Intervales (hilltop, middle slope and bottom of valley) and respective minimum percentage of forest cover where they occurred in fragmented and continuous areas; or according to IUCN threat categories (least concern species: 0%; endangered and near threatened species: 100%). We used species' minimum percentage of forest cover as the basis to define their positions in the sequence of extinctions. Family names are according to IOC World Bird List (Gill & Donsker 2018).

* Species whose minimum percentage of forest cover was derived from IUCN information.

Bird species	Bird family	Minimum percentage of forest cover
Baryphthengus ruficapillus	Momotidae	100.0
Euphonia violacea	Fringillidae	100.0
Hemithraupis ruficapilla	Thraupidae	100.0
Ilicura militaris	Pipridae	100.0
Lipaugus lanioides *	Cotingidae	100.0
Orchesticus abeillei *	Thraupidae	100.0
Orthogonys chloricterus	Mitrospingidae	100.0
Oxyruncus cristatus	Tityridae	100.0
Phibalura flavirostris *	Cotingidae	100.0
Pipile jacutinga *	Cracidae	100.0
Pteroglossus bailloni *	Ramphastidae	100.0
Saltator fuliginosus	Thraupidae	100.0
Selenidera maculirostris	Ramphastidae	100.0
Tachyphonus cristatus	Thraupidae	100.0
Tangara cyanocephala	Thraupidae	100.0
Tangara seledon	Thraupidae	100.0
Tinamus solitarius	Tinamidae	100.0
Trogon viridis	Trogonidae	100.0
Myiobius barbatus	Tityridae	66.7
Carpornis cucullata	Cotingidae	66.4
Pyrrhura frontalis	Psittacidae	66.4
Patagioenas plumbea	Columbidae	51.7
Procnias nudicollis	Cotingidae	51.7
Dacnis cayana	Thraupidae	45.6

Table D2. Continued

Pachyramphus validus	Tityridae	38.9
Ramphastos dicolorus	Ramphastidae	38.9
Thraupis cyanoptera	Thraupidae	38.9
Tityra cayana	Tityridae	38.9
Euphonia pectoralis	Fringillidae	36.5
Trogon surrucura	Trogonidae	33.3
Cacicus chrysopterus	Icteridae	30.0
Tangara desmaresti	Thraupidae	26.9
Trogon rufus	Trogonidae	26.9
Turdus flavipes	Turdidae	26.9
Brotogeris tirica	Psittacidae	25.0
Celeus flavescens	Picidae	23.4
Elaenia mesoleuca	Tyrannidae	23.4
Penelope obscura	Cracidae	23.4
Pyroderus scutatus	Cotingidae	23.4
Attila rufus	Tyrannidae	20.8
Hylophilus poicilotis	Vireonidae	20.8
Vireo olivaceus	Vireonidae	20.8
Habia rubica	Cardinalidae	15.3
Haplospiza unicolor	Thraupidae	15.3
Myiarchus swainsoni	Tyrannidae	13.0
Myiodynastes maculatus	Tyrannidae	12.0
Sittasomus griseicapillus	Furnariidae	10.8
Turdus leucomelas	Turdidae	9.6
Turdus amaurochalinus	Turdidae	6.9
Chiroxiphia caudata	Pipridae	5.1
Mionectes rufiventris	Tyrannidae	5.1
Platyrinchus mystaceus	Tyrannidae	5.1
Saltator similis	Thraupidae	5.1
Schiffornis virescens	Tityridae	5.1
Tachyphonus coronatus	Thraupidae	5.1
Trichothraupis melanops	Thraupidae	5.1
Turdus albicollis	Turdidae	5.1
Turdus rufiventris	Turdidae	5.1
Arremon flavirostris *	Passerellidae	0.0
Cacicus haemorrhous *	Icteridae	0.0
Cissopis leverianus *	Thraupidae	0.0
Elaenia flavogaster *	Tyrannidae	0.0
Stephanophorus diadematus *	Thraupidae	0.0

Table D2. Continued

Tangara sp	Thraupidae	0.0
Thraupis ornata *	Thraupidae	0.0
Turdus subalaris *	Turdidae	0.0
Zonotrichia capensis *	Passerellidae	0.0

References

Gill, F and Donsker, D. (eds). 2018. IOC World Bird List (v8.1). doi : 10.14344/IOC.ML.8.1.

Table D3. Estimates, standard error, confidence intervals (95%) and significance of breakpoints identified using linear piecewise regressions between network descriptors and proportion of habitat cover in the landscape, assuming a realistic sequence of extinctions or random extinctions of bird species.

Network descriptor	**Extinctions**	**Network**	**Breakpoint**	**Standard error**	**Confidence interval (95%)**	**Davies' test p value**
Number of species	Realistic	Hilltop	0.43	0.05	0.30–0.56	0.02
		Middle slope	0.35	0.03	0.26–0.44	0.00
		Bottom of valley	0.40	0.04	0.30–0.50	0.01
		Combined	0.39	0.05	0.27–0.51	0.01
	Random	Hilltop	0.43	0.00	0.42–0.43	0.00
		Middle slope	0.37	0.00	0.37–0.37	0.00
		Bottom of valley	0.40	0.00	0.39–0.40	0.00
		Combined	0.37	0.00	0.36–0.37	0.00
Number of interactions	Realistic	Hilltop	0.44	0.06	0.28–0.61	0.04
		Middle slope	0.40	0.07	0.22–0.58	0.03
		Bottom of valley	0.41	0.02	0.36–0.45	0.00
		Combined	0.41	0.04	0.32–0.50	0.00
	Random	Hilltop	0.43	0.00	0.43–0.44	0.00
		Middle slope	0.38	0.00	0.38–0.39	0.00
		Bottom of valley	0.40	0.00	0.40–0.41	0.00

		Combined	0.39	0.00	0.38–0.39	0.00
Connectance	Realistic	Hilltop	0.38	0.05	0.26–0.50	0.01
		Middle slope	0.28	0.01	0.25–0.31	0.00
		Bottom of valley	0.36	0.06	0.22–0.51	0.03
		Combined	0.32	0.02	0.27–0.36	0.00
	Random	Hilltop	0.37	0.00	0.37–0.38	0.00
		Middle slope	0.33	0.00	0.33–0.34	0.00
		Bottom of valley	0.36	0.00	0.35–0.36	0.00
		Combined	0.34	0.00	0.33–0.34	0.00
Nestedness (NODF)	Realistic	Hilltop	0.44	0.15	0.05–0.82	0.44
		Middle slope	0.32	0.02	0.27–0.37	0.00
		Bottom of valley	0.36	0.06	0.22–0.51	0.03
		Combined	0.31	0.03	0.22–0.40	0.01
	Random	Hilltop	0.38	0.03	0.33–0.43	0.00
		Middle slope	0.33	0.02	0.30–0.36	0.00
		Bottom of valley	0.40	0.02	0.36–0.44	0.00
		Combined	0.35	0.01	0.33–0.36	0.00
Mean degree of birds	Realistic	Hilltop	0.43	0.04	0.33–0.53	0.48
		Middle slope	0.23	0.02	0.19–0.27	0.00
		Bottom of valley	0.34	0.07	0.17–0.50	0.07

		Combined	0.29	0.03	0.20–0.38	0.00
	Random	Hilltop	0.43	0.00	0.43–0.43	0.61
		Middle slope	0.54	0.21	0.12–0.96	0.50
		Bottom of valley	0.69	1.25	-1.77–3.15	1.00
		Combined	0.45	0.49	-0.52–1.41	0.95
Mean degree of plants	Realistic	Hilltop	0.42	0.03	0.35–0.49	0.00
		Middle slope	0.41	0.05	0.27–0.54	0.02
		Bottom of valley	0.38	0.03	0.29–0.47	0.00
		Combined	0.42	0.03	0.35–0.49	0.00
	Random	Hilltop	0.42	0.00	0.42–0.43	0.00
		Middle slope	0.38	0.00	0.37–0.38	0.00
		Bottom of valley	0.39	0.00	0.39–0.40	0.00
		Combined	0.38	0.00	0.38–0.39	0.00

APPENDIX E. Impacts of realistic extinctions on the three frugivory networks

Here we present the results of the simulations of bird species extinctions driven by habitat loss on the structure of the three studied frugivory networks: hilltop (Fig. E1), middle slope (Fig. E2) and bottom of valley (Fig. E3); and robustness of such networks to different models of species extinctions (Fig. E4).

Hilltop

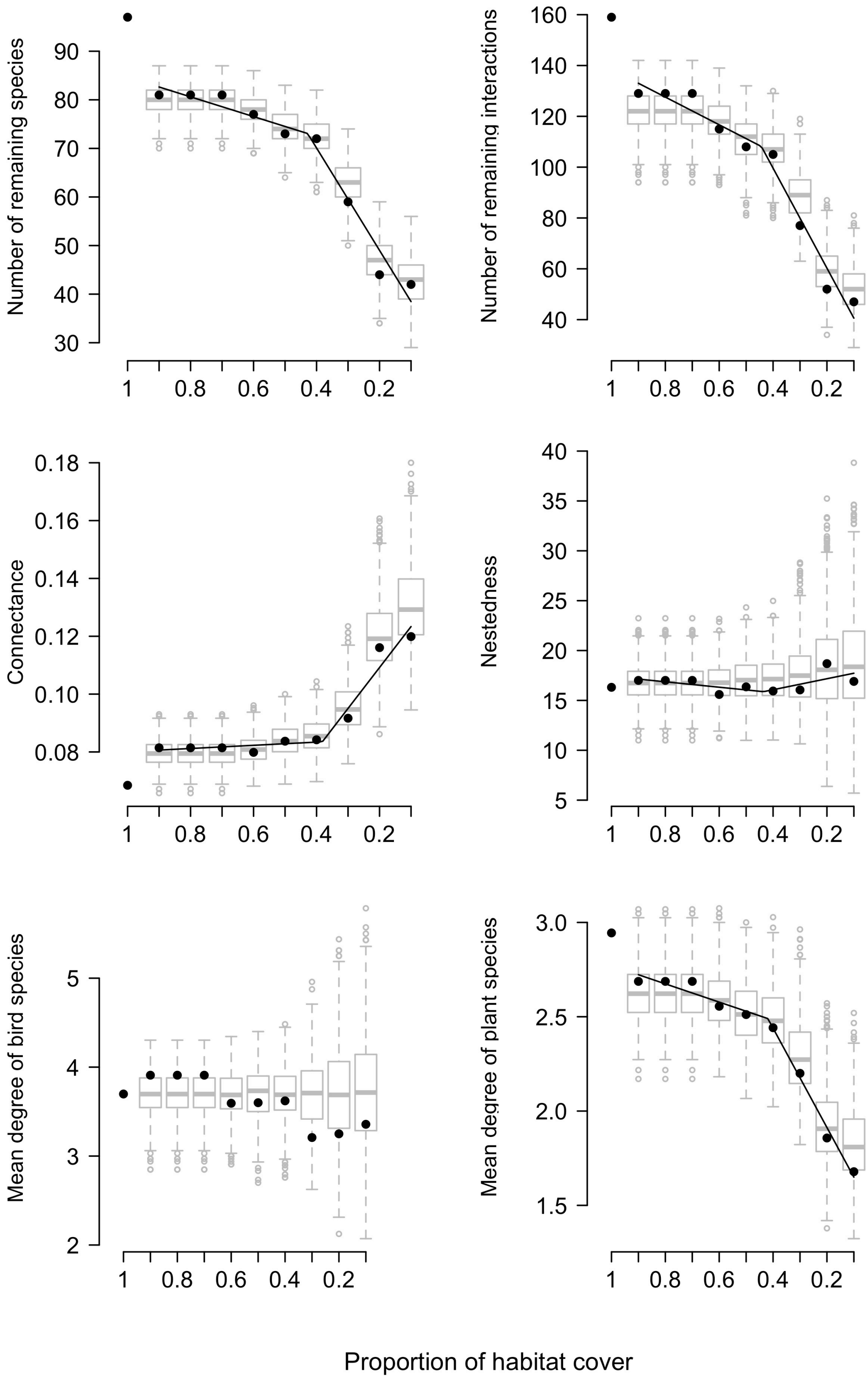

Number of remaining species
Number of remaining interactions
Connectance
Nestedness
Mean degree of bird species
Mean degree of plant species
Proportion of habitat cover

Figure E1. Effects of habitat loss on the structure of the hilltop frugivory network. Black dots depict structural values of the networks as birds, and secondarily plants, were lost in simulations of habitat destruction. Gray boxplots represent results from random deletions of bird species. Solid black lines are the fitted linear models with breakpoints, representing the threshold in the response of network parameters to habitat loss.

Middle slope

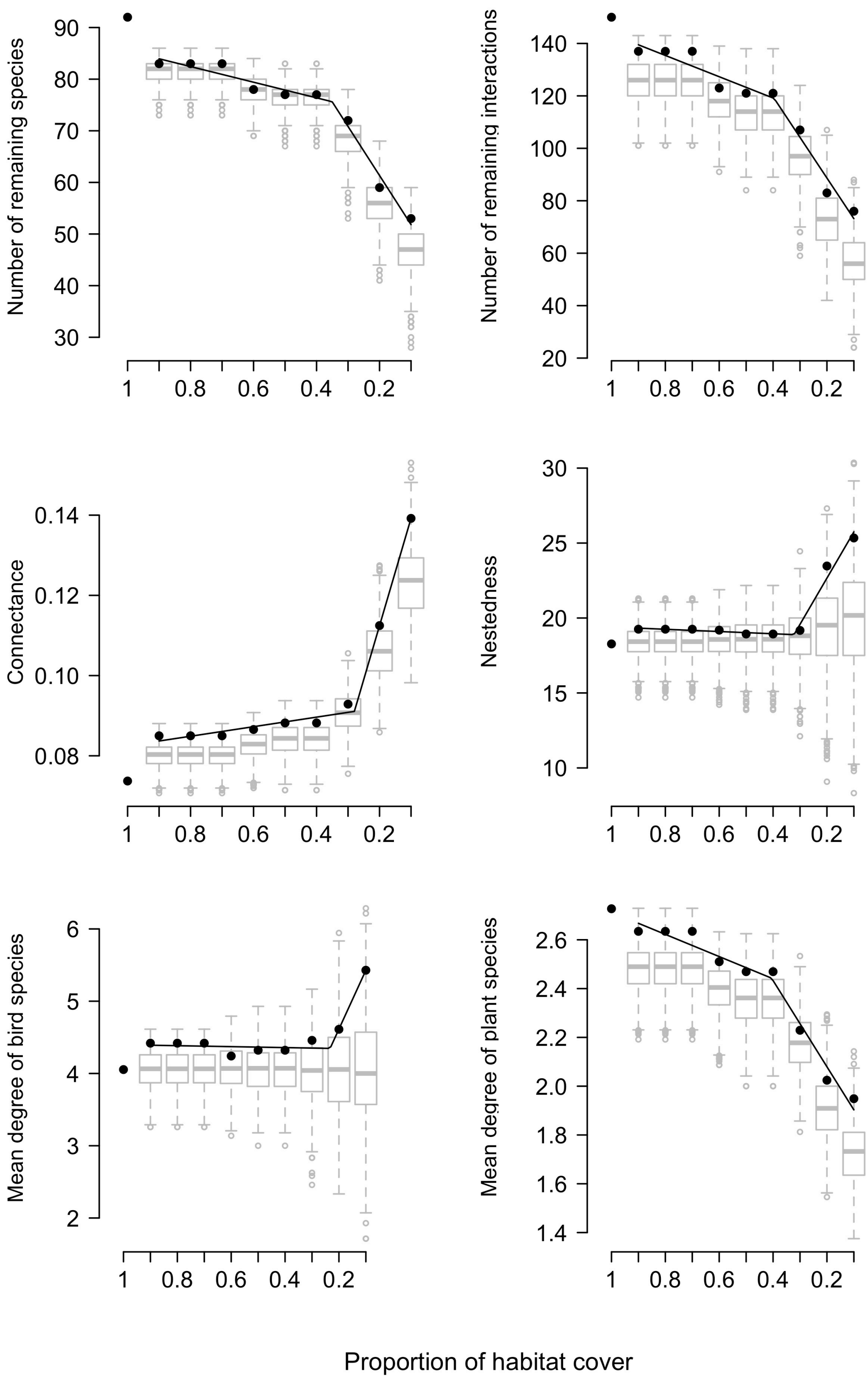

Figure E2. Effects of habitat loss on the structure of the middle slope frugivory network. Black dots depict structural values of the networks as birds, and secondarily plants, were lost in simulations of habitat destruction. Gray boxplots represent results from random deletions of bird species. Solid black lines are the fitted linear models with breakpoints, representing the threshold in the response of network parameters to habitat loss.

Bottom of valley

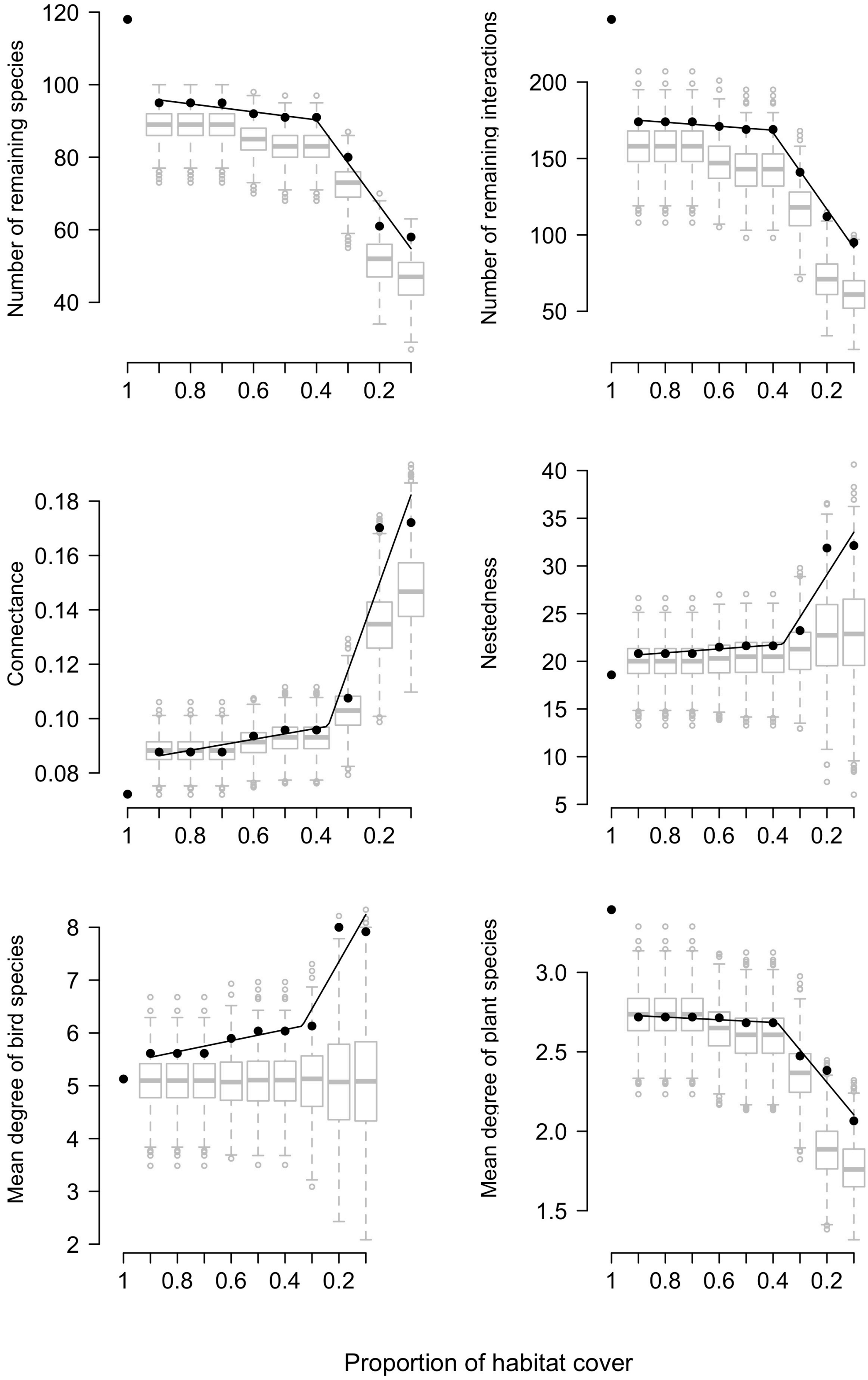

Figure E3. Effects of habitat loss on the structure of the bottom of valley frugivory network. Black dots depict structural values of the networks as birds, and secondarily plants, were lost in simulations of habitat destruction. Gray boxplots represent results from random deletions of bird species. Solid black lines are the fitted linear models with breakpoints, representing the threshold in the response of network parameters to habitat loss.

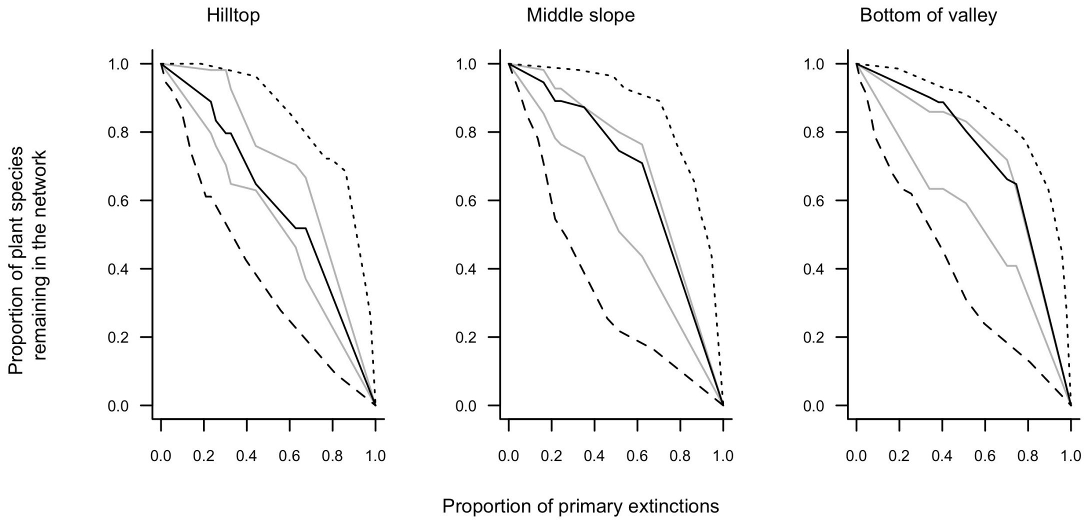

Figure E4. Robustness of the three studied frugivory networks (hilltop, middle slope and bottom of valley). Solid black lines depict the tolerance curve for the realistic sequence of bird extinctions following habitat loss. Gray lines are the 2.5% and 97.5% quantiles of the areas under curves produced by the random sequences of extinctions. Dashed black lines correspond to the tolerance curve for the removal of the most-linked to least-linked bird species. Dotted black lines correspond to the tolerance curve for the removal of the least-linked to most-linked bird species.

APPENDIX F. Number of interactions of bird and plant species

Here we show the distribution of the number of interactions (degree) of bird and plant species (Fig. F1) and the relationship between the minimal forest cover where each bird species was recorded and the degree of each bird species (Fig. F2).

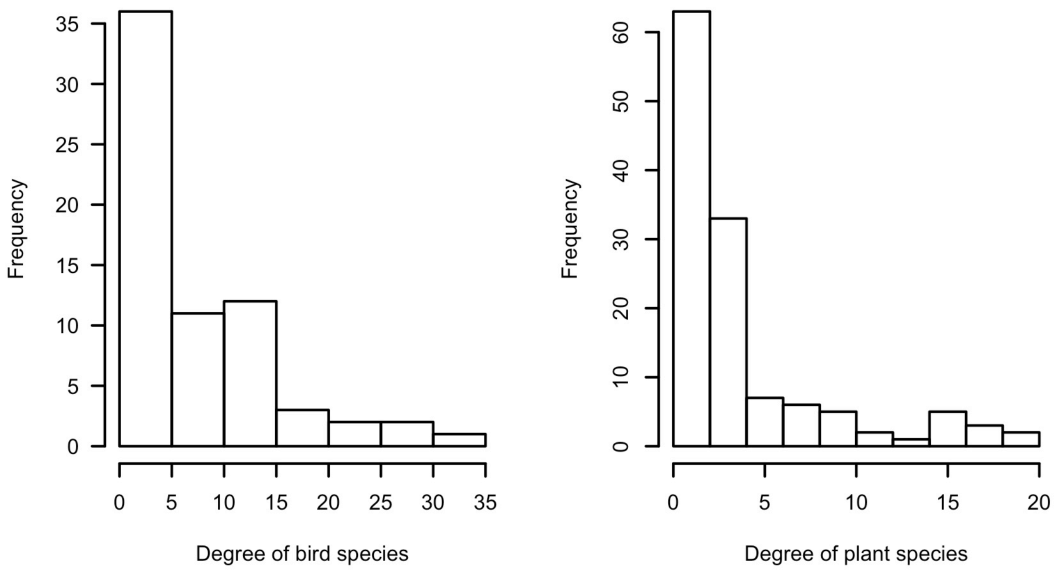

Figure F1. Distribution of the degree (number of interactions) of bird and plant species.

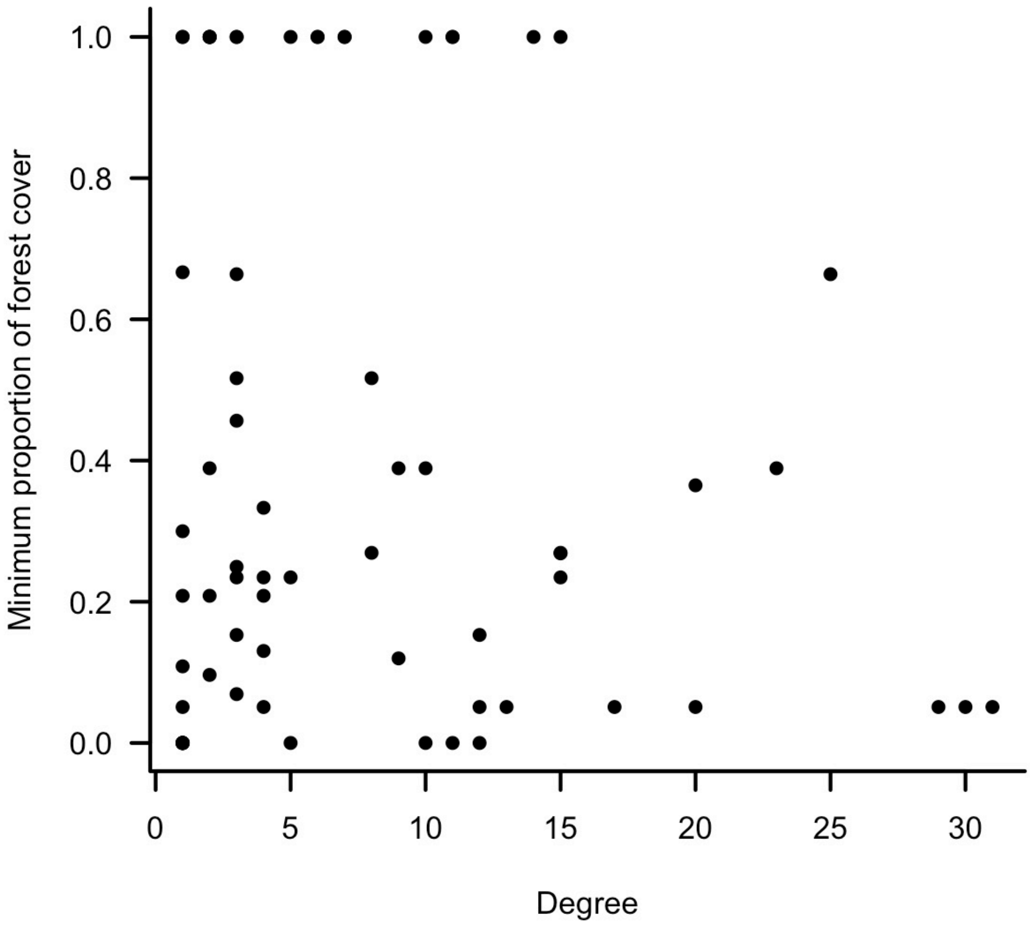

Figure F2. Relationship between minimum proportion of forest cover where each bird species was recorded and the number of interactions (degree) of each bird species. Pearson correlation coefficient = -0.15, p=0.23.